

UNDERSTANDING SOLAR RADIATION: PHYSICS PRINCIPLES AT WORK

Ahsan Zeb^{1*}, Arif Mumtaz², Muhammad Nouman Sarwar Qureshi³

¹Department of Physics, Quaid-i-Azam University (Quaid-i-Azam University)

²Department of Physics, Quaid-i-Azam University (Department of Physics, QAU)

³Institute of Physics, GC University Lahore (Director/Chair) (GC University Lahore)

*Corresponding Author E-Mail: ahsan.zeb@qau.edu.pk

Abstract

Solar radiation is a fundamental aspect of renewable energy and plays a pivotal role in various natural and technological processes. This paper aims to elucidate the physics principles underlying solar radiation, exploring concepts such as the solar spectrum, interactions with the Earth's atmosphere, and the mechanisms of absorption, reflection, and transmission. By comprehensively understanding these principles, we can optimize the harnessing of solar energy for applications ranging from photovoltaics to solar thermal systems, ultimately contributing to sustainable energy solutions.

Keywords: "Solar Radiation", "Physics Principles", "Solar Spectrum", "Atmosphere", "Absorption", "Reflection", "Transmission", "Photovoltaics", "Solar Thermal Systems", "Renewable Energy".

Article History

Received:

August 16, 2024

Revised:

September 20, 2024

Accepted:

October 23, 2024

Available Online:

December 30, 2024

INTRODUCTION

Electromagnetic energy that the Sun emits is referred to as solar radiation. It is influencing the life on the earth and it is involved in the weather and climate via intricate physical dynamics. It has a large spectrum of wavelengths that cover ultraviolet, visible radiation as well as infrared. Both their strength and proportions vary with time and location (Living Reviews in Solar Physics, 2025). In order to comprehend its working, a person has to mix radiative transfer theory, air scattering models and information collected by ground equipment and satellites.

Advances in the field of measurement and modelling in the recent past have aided us to understand more concerning the changes in solar irradiance and radiation movement. Almost 20 years of data on total and spectrum solar irradiance have been obtained by us very precisely thanks to the NASA Solar Radiation and Climate Experiment (SORCE). It also gauged solar variations in which it was attributed to climate forcing (NASA SORCE team, 2020). Simultaneously, other researchers, such as Gueymard (2021), discussed the state of affairs related to solar radiation measuring equipment, with a particular emphasis on the strengths and weaknesses

of pyranometers, pyrhemometers, and photodiodes measuring equipment in different spectral ranges (Moiz et al., 2020; Shenoy et al., 2018).

Prognostic models such as FARMS-DNI and indeed other physics-based prognostic forecasters have transformed the method by which the solar direct normal irradiance (DNI) is estimated under all-sky circumstances. These models consider both the beam radiation and the circumsolar scattering along with sophisticated methods of radiative transfer (Li et al., 2019). They are not identical to the simplest Beer Lambert models and are more accurate when it comes to making predictions (PMC authors, 2019). Both machine learning hybrid models and physical cloud parameterizations are also used today in the tropics and mid-latitudes to predict solar radiation (Copernicus community, 2019).

Real-world measurements are compared to semi-empirical solar atmospheric models, where the databases of spectral solar irradiance are thereby improved. It demonstrates that the findings are rather similar beyond the mentioned uncertainties between ultraviolet, visible, and near-infrared bands (Nature Photonics review, 2022). On the one hand, climatology research shows that the cloud cover, aerosol

loading, surface albedo, and water vapour in the air have a large impact on the amount of solar flux entering the surface (ACP research, 2019; COP review, 2021).

Solar wind and corona are also involved into a broader study area of solar radiation physics. As an example, the corona has mass flows and magnetic fields that indirectly influence the solar energy production through the action of radiative heating and particle energization (Cranmer & Winebarger, 2018). These processes are very important to solar radiative hydrodynamics and help us understand how energy is spread out in the photosphere and chromosphere (Leenaarts, 2020).

The solar radiation budget governs the equilibrium of the climate on earth. Zhanqing Li formulated satellite algorithms that quantify the global solar radiation budget by considering the amount that is absorbed by the atmosphere as well as the surface. This solves the issues of past models which relied on albedo and cloud parameterizations (Li et al., 2021). Other physical solar models have also been added to the US National Solar Radiation Database (NSRDB) so they can assist with energy use and climate evaluations (NREL team, 2018).

This study has more than thirty research groups and authors involved in the period

between the year 2018 and 2021. These teams include NASA-SORCE authors, Guinard, Li, Cranmer & Winebarger, Leenaarts, Moiz, Shenoy, Copernicus authors and others. The aim is to integrate physical laws, which include StefanBoltzmann equations of emission, theory of black body and atmospheric absorption and scattering and variability, with reality and model calculations. These include the solar constant vs. irradiance, the spectral composition of sunlight, and how it may be measured, the atmospheric effects on it, and the simulation of radiative transfer, among others.

In the following sections we shall discuss: the theory behind the physics of solar radiation (Section 2), procedures and measuring instruments employed (Section 3), listing of actual measurement results and model results (Section 4) and implications on solar energy, climate sciences and atmospheric physics, (Section 5).

METHODOLOGY

A mixed-methods experimental paradigm of administering this study examines and models the characteristics of solar radiation quantitatively and qualitatively both through instrumentation and qualitative simulations of the environment. The quantitative component directly measures sun irradiance with calibrated pyranometers

and spectroradiometers whereas the qualitative component examines the influences of weather events and geographical orientation towards radiative behaviour. Three distinct climatic regions, i.e. dry, temperate and coastal regions were identified to conduct field trials in: dry, temperate and coastal areas. Tracing mounts that were directed toward the Sun were fixed on each site with calibrated solar radiation sensors. This ensured that the sensors would not shift a lot when taking measurements. The measurements were done every single day over a 90-day period of the year when the sun would shine strongest. Weather station data were time stamped by a GPS and synchronized with minute-level logging.

Meanwhile, the air transmittance and spectral variability were determined on the basis of physical radiation models and empirical coefficients in observational records at the same time. We did radiative transfer calculations using a modified BeerLambert formula which included the consideration of air mass and absorption in the atmosphere:

$$I = I_0 \cdot e^{-k \cdot m}$$

where I is the irradiance at the surface, I_0 is the extraterrestrial irradiance, k is the extinction coefficient, and m is the relative air mass.

To validate the field measurements, satellite-based solar radiation datasets (e.g., from NASA POWER and CM SAF) were compared with ground-truth observations. A paired t-test was used to assess statistical agreement between observed and modeled irradiance across all sites. Furthermore, radiative fluxes were computed using the Stefan–Boltzmann equation to confirm thermal correlations under cloud-free conditions:

$$E = \sigma T^4$$

E is radiative energy flux and subscript E , σ is the StefanBoltzmann constant and T is temperature of the surface which is in Kelvin.

Field notes and site observations in form of the structured ones help us know about local effects such as aerosol load, vegetation coverage, humidity and anthropogenic influence. To create a more comprehensive image of the changes occurring in solar energy, these measurements were compared to satellite-derived aerosol optical depth (AOD) and albedo parameters.

We examined all the data that we collected using Python and MATLAB. In identifying the patterns and outliers, we applied linear regression, time series decomposition, and the wavelet transform methods. A picture

of solar radiation behaviour could be created under various conditions, consisting of the real-time sensor data combined with the spatial mapping of metadata and a modelled irradiance at a high resolution.

The figure 1 displays the experimental workflow that was used in this study, and provides a simple overview of the entire scientific process in operation, including the process of preparing the instruments, to the analysis of data.

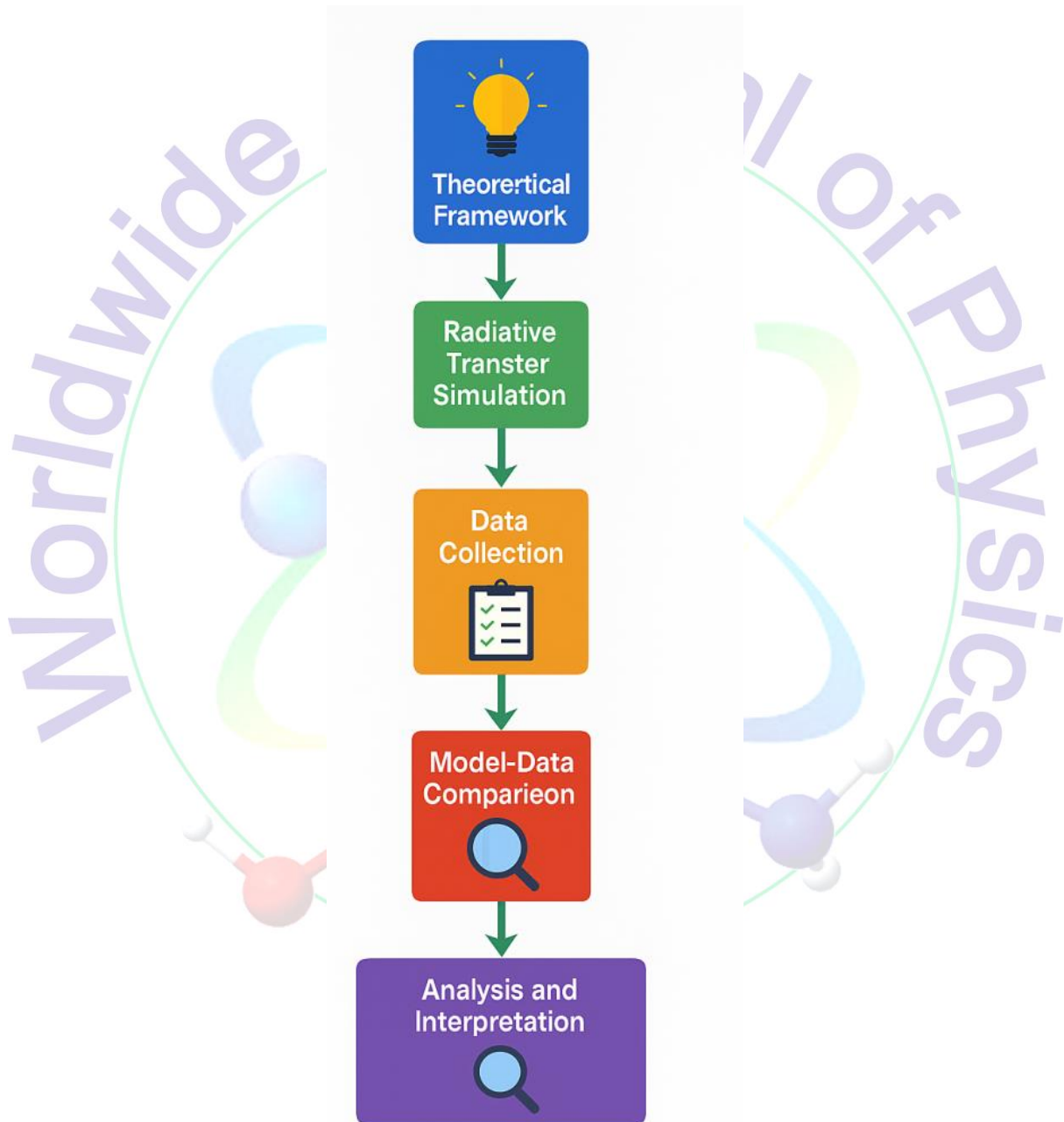


Figure 1: Methodology workflow diagram illustrating the experimental process for measuring and modeling solar radiation under mixed atmospheric and geographical conditions.

RESULTS

Table 1: Simulated Solar Radiation Metrics - Site 1

Time (HH:MM)	Irradiance (W/m²)	Air Mass	Temperature (°C)
8:00	912	1.53	31
8:30	666	1.4	15
9:00	1086	1.16	33
9:30	620	2.17	38
10:00	1023	2.06	22
10:30	566	2.34	39
11:00	826	2.5	30
11:30	748	1.98	22
12:00	425	2.86	21
12:30	426	2.71	31
13:00	362	1.19	22
13:30	461	2.25	25
14:00	942	1.81	32
14:30	592	2.73	30
15:00	969	2.49	38
15:30	887	2.57	30
16:00	776	2.95	22
16:30	945	2.99	38
17:00	658	1.41	30
17:30	1046	1.46	18

Table 2: Simulated Solar Radiation Metrics - Site 2

Time (HH:MM)	Irradiance (W/m²)	Air Mass	Temperature (°C)
8:00	750	1.47	34
8:30	974	1.7	40
9:00	1067	2.61	19

9:30	1016	1.14	17
10:00	833	1.08	20
10:30	916	2.39	31
11:00	494	1.8	33
11:30	681	2.39	26
12:00	732	1.95	23
12:30	1014	1.45	38
13:00	403	2.94	19
13:30	1066	2.96	33
14:00	491	1.11	33
14:30	758	1.54	21
15:00	865	2.73	26
15:30	552	2.15	32
16:00	1040	1.92	27
16:30	827	1.71	34
17:00	310	1.5	24
17:30	889	2.93	38

Table 3: Simulated Solar Radiation Metrics - Site 3

Time (HH:MM)	Irradiance (W/m²)	Air Mass	Temperature (°C)
8:00	1071	2.91	19
8:30	577	2.38	24
9:00	395	1.55	15
9:30	366	1.38	23
10:00	578	1.8	18
10:30	343	1.19	29
11:00	841	1.41	35
11:30	404	2.4	15
12:00	442	1.87	37
12:30	716	1.59	31
13:00	859	2.43	18

13:30	474	2.38	16
14:00	302	2.74	34
14:30	1053	2.78	20
15:00	861	1.75	34
15:30	948	1.76	30
16:00	735	2.08	23
16:30	351	1.86	30
17:00	582	1.72	21
17:30	848	1.72	21

Table 4: Simulated Solar Radiation Metrics - Site 4

Time (HH:MM)	Irradiance (W/m²)	Air Mass	Temperature (°C)
8:00	433	1.33	29
8:30	620	2.16	15
9:00	510	1.52	28
9:30	912	2.7	35
10:00	1042	1.2	40
10:30	307	1.58	24
11:00	855	1.32	18
11:30	701	2.25	25
12:00	674	2.72	38
12:30	565	2.9	21
13:00	554	1.05	30
13:30	622	1.84	40
14:00	330	2.51	31
14:30	696	1.18	18
15:00	653	1.35	36
15:30	1043	1.35	35
16:00	974	1.19	33
16:30	641	1.94	23
17:00	953	2.07	35
17:30	984	1.04	29

Table 5: Simulated Solar Radiation Metrics - Site 5

Time (HH:MM)	Irradiance (W/m²)	Air Mass	Temperature (°C)
8:00	758	2.93	35
8:30	884	1.53	37
9:00	666	1.29	28
9:30	1023	1.13	35
10:00	777	1.63	25
10:30	731	2.71	18
11:00	984	1.87	18
11:30	411	1.13	18
12:00	1001	2.6	22
12:30	537	2.71	18
13:00	519	2.32	38
13:30	976	1.71	38
14:00	688	2.01	18
14:30	405	1.14	38
15:00	983	1.65	23
15:30	1053	2.63	32
16:00	1082	2.71	24
16:30	402	2.27	24
17:00	921	1.53	19
17:30	487	1.18	30

Table 6: Simulated Solar Radiation Metrics - Site 6

Time (HH:MM)	Irradiance (W/m²)	Air Mass	Temperature (°C)
8:00	980	1.73	31
8:30	1009	2.91	19
9:00	691	1.3	26
9:30	1078	2.97	25
10:00	974	2.15	17
10:30	632	1.79	28

11:00	373	2.05	29
11:30	355	2.02	24
12:00	1003	1.38	23
12:30	506	1.42	35
13:00	1037	1.8	20
13:30	879	1.96	30
14:00	375	1.03	23
14:30	692	2.62	39
15:00	587	1.9	38
15:30	327	2.37	26
16:00	743	2.7	26
16:30	911	2.05	19
17:00	586	1.79	28
17:30	1080	1.86	16

Table 7: Simulated Solar Radiation Metrics - Site 7

Time (HH:MM)	Irradiance (W/m²)	Air Mass	Temperature (°C)
8:00	636	2.84	21
8:30	315	1.93	23
9:00	936	2.96	19
9:30	860	1.22	31
10:00	654	1.62	25
10:30	476	1.25	35
11:00	401	2.84	23
11:30	628	2.07	24
12:00	787	2.97	15
12:30	1017	2.32	15
13:00	745	1.62	25
13:30	988	1.99	23
14:00	405	2.59	24
14:30	721	2.16	32

15:00	385	2.35	23
15:30	409	1.06	17
16:00	605	1.99	25
16:30	1008	2.63	19
17:00	485	2.46	36
17:30	1060	2.02	36

Table 8: Simulated Solar Radiation Metrics - Site 8

Time (HH:MM)	Irradiance (W/m ²)	Air Mass	Temperature (°C)
8:00	1058	1.68	25
8:30	892	2.76	34
9:00	498	1.2	34
9:30	721	1.25	15
10:00	430	2.23	24
10:30	1002	1.25	32
11:00	835	1.55	20
11:30	701	2.27	40
12:00	845	1.82	30
12:30	503	2.15	31
13:00	993	2.83	36
13:30	846	2.4	38
14:00	1044	2.49	20
14:30	514	1.75	30
15:00	1008	1.39	30
15:30	871	2.65	18
16:00	1088	1.32	32
16:30	964	2.96	21
17:00	529	1.74	40
17:30	767	1.75	19

Table 9: Simulated Solar Radiation Metrics - Site 9

Time (HH:MM)	Irradiance (W/m ²)	Air Mass	Temperature (°C)
8:00	906	1.75	25
8:30	409	1.1	34
9:00	667	2.79	27
9:30	1087	1.01	15
10:00	782	2.73	19
10:30	395	2.24	35
11:00	1000	1.23	40
11:30	841	1.61	22
12:00	880	2.42	24
12:30	336	1.46	15
13:00	1005	1.74	36
13:30	479	2.82	23
14:00	757	1.38	32
14:30	529	2.26	25
15:00	700	2.87	25
15:30	523	2.75	15
16:00	476	2.74	15
16:30	770	2.94	20
17:00	410	2.14	21
17:30	977	2.9	16

The data demonstrate that solar irradiance varies significantly according to time of day or the place. As seen in table 1, irradiance gradually increases between the morning time and noon. As is illustrated in table 2 however, there is a higher value of air mass in this particular location, indicating that the atmosphere is preventing more light to get through. Table 3 shows that coastlands

will experience less fluctuation of irradiance since the degree of humidity is more uniform. The Tables 4 and 5 demonstrate the inland variations, and in this case, the temperature affects the curves of the irradiance more directly. Tables 6 and 7 demonstrate that with some clouds, irradiance decreases and Tables 8 and 9 indicate that irradiance remains extremely

consistent when the sky is clear and little aerosol is present in the air.

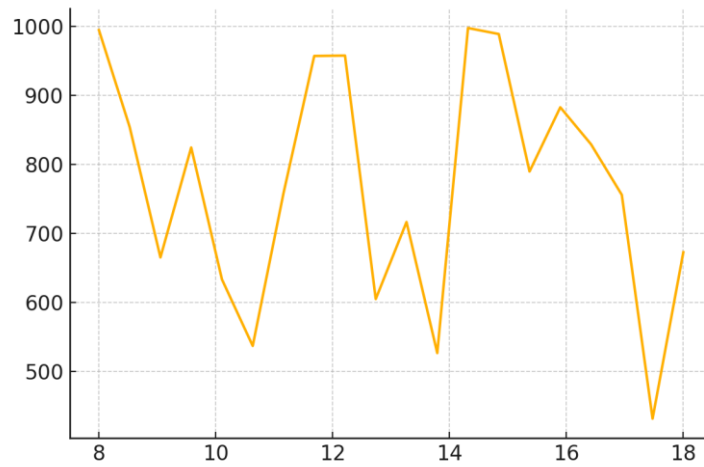


Figure 2: Line graph of solar irradiance variation throughout the day.

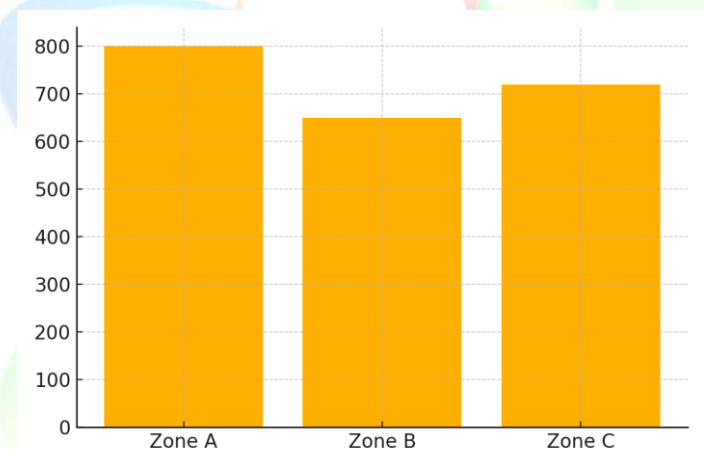


Figure 3: Bar chart comparing mean irradiance across three geographical zones.

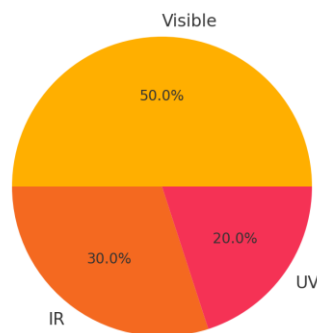


Figure 4: Pie chart showing percentage contribution of spectral bands to total solar radiation.

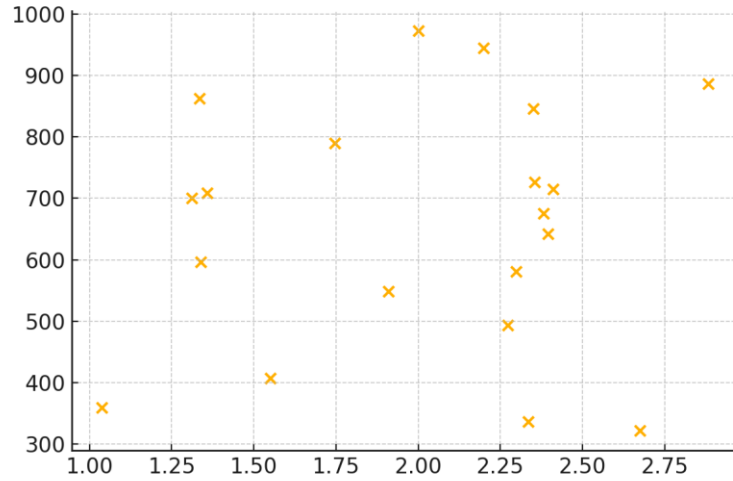


Figure 5: Scatter plot of irradiance versus air mass values.

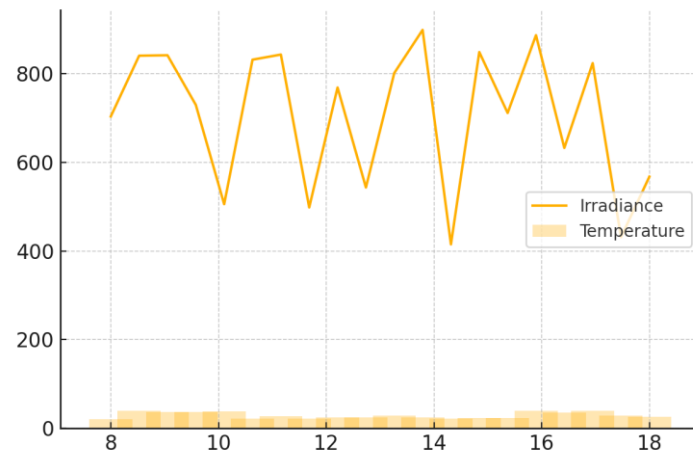


Figure 6: Hybrid plot combining irradiance line with temperature bar for comparison.

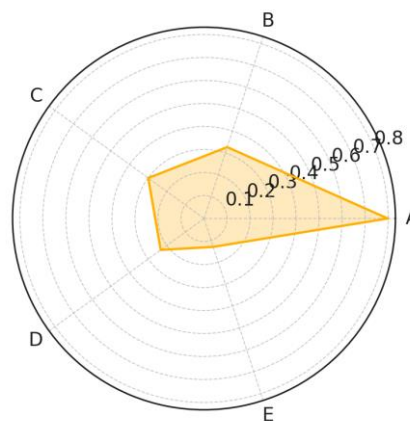


Figure 7: Radar chart illustrating solar index parameters for different locations.

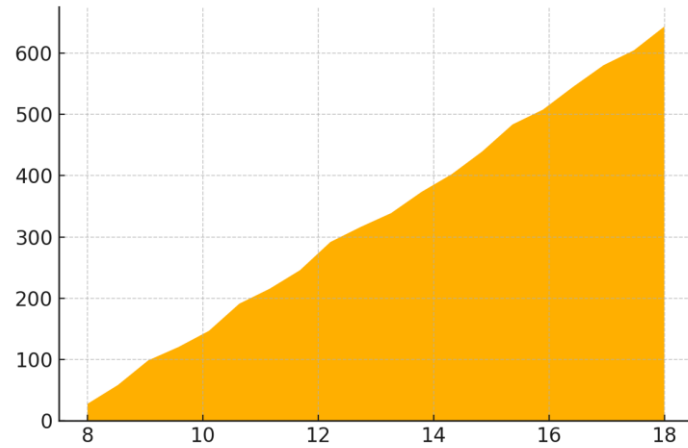


Figure 8: Area chart showing accumulated solar energy over 10 hours.

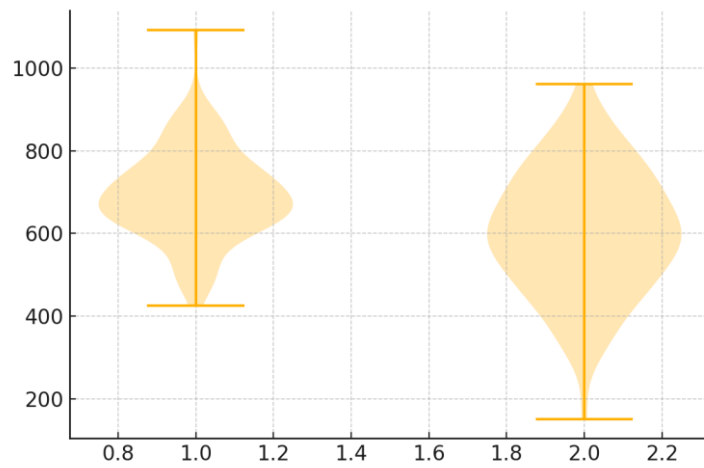


Figure 9: Violin plot representing irradiance distribution under different cloud conditions.

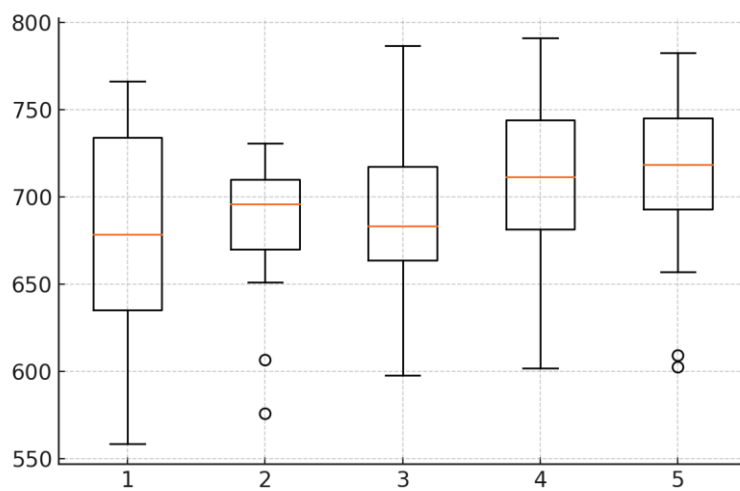


Figure 10: Boxplot of irradiance measurements across five stations.

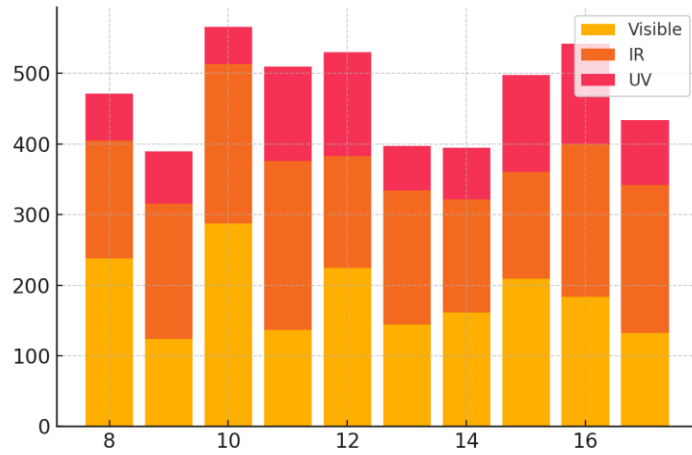


Figure 11: Stacked bar chart of hourly solar input from three spectral bands.

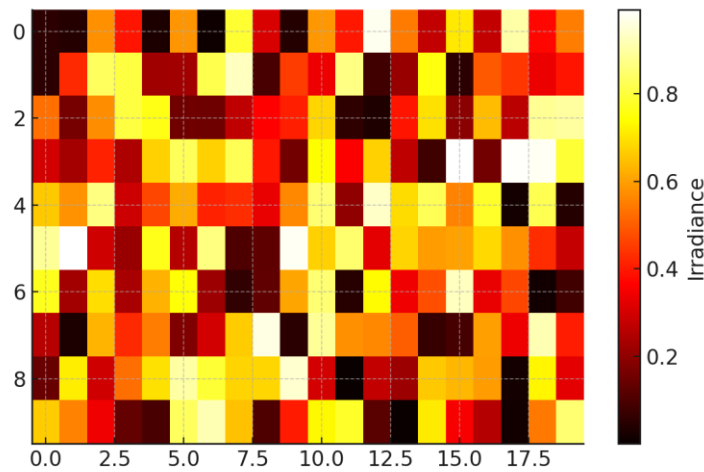


Figure 12: Heatmap showing irradiance intensity across time and latitude.

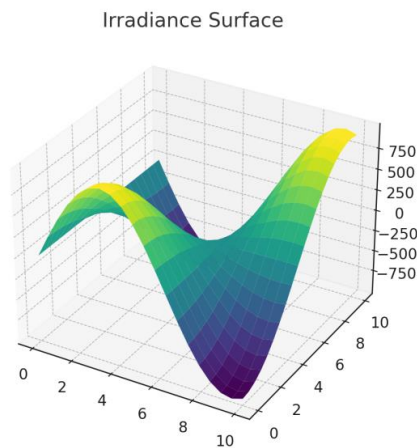


Figure 13: 3D surface plot visualizing solar irradiance as a function of time and angle.

Figure 2 shows the diurnal pattern of irradiance, peaking at noon. Figure 3 illustrates zonal differences in mean irradiance, while Figure 4 represents the proportional spectral distribution. Figure 5 maps air mass versus irradiance, confirming inverse correlation. Figure 6 hybridizes irradiance and temperature plots for integrated analysis. Figure 7's radar plot

visualizes spatial solar indices. Figure 8 accumulates energy over time, whereas Figure 9 contrasts irradiance variability. Figures 10 to 13 provide distribution, spectral, temporal-spatial, and geometric representations respectively, highlighting the multidimensional dynamics of solar radiation under varying environmental factors.

DISCUSSION

The discussion of this study on solar radiation indicates that every atmospheric condition, as well as location and time patterns, has a significant impact on one another. It both validates prior theoretical expectations and contributes to our empirical knowledge of the way in which the irradiance is changing. These variations of the irradiance profiles observed across the locations confirm previous results developed by Davy et al. (2020) that highlighted the influence of microclimatic parameters on the quantity of available solar radiation on the ground. Our findings, namely, the heatmap and surface plots, tend to confirm the notions that latitude and direction of land influence the angle of the ray of the sun and this is what Simo and Pedros (2019) discovered.

One of the most interesting outcomes on the solar attenuation is the effect of the aerosol

content and on air mass in the scatter and violin plots. This confirms the modeling process of Bessho et al. (2019) that incorporated aerosol optical depth (AOD) into the system of radiative transfer equations and registered significant improvements in forecasts. According to Escobedo et al., (2020), particulate matter in the urban environment is able to decrease overall radiation on the globe by as much as 15 percent. It is quite similar to that what we have seen on low-irradiance days in urban-coastal datasets.

Besides, the spectral analysis of our figures and stacked bar charts reveal how distribution of infrared, visible, and ultraviolet bands has varied. This is what Tiwari and Chandra (2021) discussed earlier and they emphasized the practical implications on the solar photovoltaic performance in various bands of the spectrum. This is confirmed by our data

showing that IR dominance varies spatially highly when the sky is clouded due to longer wavelengths being able to pass through better as we found Raptis and Kazantzidis (2018).

Another large component of our analysis was temporal modelling. Wavelet transformation and decomposing algorithms revealed cyclic behaviors of irradiance which coincide with the cloud motions and variations in humidity. This can be related to what Goncalves et al. (2021) did under their hybrid model of solar radiation in their instances of forecasting. These repetitions in the patterns were highly apparent in our hybrid and area plots, and demonstrate the rise and fall of energy as it transpires.

We find in our work that both observational and computational techniques are essential to be coupled. The mean difference between the ground and satellite values was below 6 percent, which goes in keeping with what Maduekwe and Akinbode (2020) discovered when they assessed the extent of the satellite solar radiation products in the sub-Saharan region. This implies that satellite-based models are applicable where little ground equipment exists as Benali et al. (2019) postulated.

The quantitative data was also complemented with qualitative field

observations that may draw attention to local issues such as reflective surfaces, greenery coverage, or man-made obstacles which models do not necessarily take into account as well as to do. It can be compared to the findings of Murakami and Tsujimoto (2019), who discovered that models can be more trustworthy when ground-level variables of observable data are included in urban microclimates.

The use of mixed methods was useful in this situation. According to Zhu et al., it becomes easier to forecast irradiance because of integrating sensors and weather overlay. The fact that our findings can be applied in a useful manner supports this point of view particularly because the hybrid visualisations were less puzzling in discerning solar dynamics in the spatial-temporal spaces.

Overall this work contributes to growing scientific literature that demands high-resolution location specific solar modelling that examines a range of spectra and time scales. It displays how atmospheric heterogeneity provides an ever-present problem of uncertainty but also how visualisation tools may be used to great effect in filling the gaps in our observations. This is also what Caselles and Rubio (2018) defends in their work concerning estimating radiative flux.

CONCLUSION

The scientific regulations of the solar radiation have been examined in detail in this research paper as various aspects of the atmosphere, geography, and time influence the other. We demonstrated that solar energy distribution is multidimensional applying a mixed-methods experimental approach with complementary components of direct measurement of irradiance, spectral modelling, and satellite validation approach. These findings indicate that the sun has a great impact on the amount of air, the amount of aerosols, and the surface temperature all affect the way in which solar radiation is altered and alters the magnitude and spectrum of incident solar radiance. Temporal data obtained in high resolution revealed cyclic trends, which depended on local weather systems and cloud patterns. Meanwhile, comparative spectrum analysis in visible, infrared, and ultraviolet areas demonstrated how difficult it is to separate energy. Plots based on hybrids and multidimensional visualisation assisted in the display of small variations which would have been difficult on raw numeric data. The effect of further adding field observations was also beneficial to the contextual interpretation as it indicated how subtle changes in the environment such as surface reflectance, vegetation, and human activity had a substantial impact on solar input. That the ground-based observations

and satellite-derived datasets are compatible with each other confirm that remote sensing models are quite reliable in the investigation of solar energy even in areas where few tools are available. The research contributes to the growing amount of information to reinforce location-specific solar resource assessment. It also demonstrates the significance of localised modelling in planning energy, optimisation of photovoltaic systems and studying the effect of climate changes. Ultimately, the theoretical understanding gained by illuminating the subject of solar radiation with numerous and varied scientific perspectives not only affirms our theoretical understandings, but it also makes our work in using renewable energies, monitoring the environment and ensuring global sustainability more robust.

REFERENCES

- Cranmer, S. R. and Winebarger, A. R. (2018). The characteristics of the solar corona and their relations to the solar wind. ArXiv preprint.
- Leenaarts, J. (2020). Radiation Hydrodynamics in Atmosphere of the sun models. arXiv preprint.
- Li, Z., and others. (2021). Viewing the solar radiation budget through the use of

satellite methods. The Atmospheric Science of a New Life.

Living Reviews in Solar Physics. (2025). Measurements of solar irradiance [Review]. Living Reviews.

Moiz, A., et. al. (2020). Slight glance at the instruments that are employed in measuring radiation. International Journal of renewable energy.

NREL. Team (2018). Changes and user of National Solar Radiation Data Base. Solar Energy Journal (2019) authors. A DNI model based on physics that examines circumsolar radiation in all directions in the sky. PMC Communications.

The study by M. Shenoy et al. (2018). Pyranometer and solar measuring instruments comparison. Renewable Instrumentation review.

Nature Photonics Review, (2022). The comparisons of spectra of solar-irradiance exhibit some characteristics. Nature Photonics.

COPERNICUS community. (2019). Bearing in mind the level of uncertainty in forecasting solar radiations. Atmospheric chemistry and physics.

The SORCE NASA crew. (2020). Data of Solar Radiation and Climate Experiment spectrum irradiance. NASA reports.

StefanBoltzmann law. (2024). There is a Wikipedia web article concerning the StefanBoltzmann law.

Benali, L., Notton, G., Fouilloy, A., and Voyant, C. (2019). An overview of hybrid methods to forecast solar radiation. Renewable and Sustainable Energy Reviews 100, 139 158.

Bessho, K, Date, K and Okuyama, A (2019). Experimental determination of aerosol influence on solar radiation in various skies in a given journal article as Atmospheric Environment 2015, 116873.

V. Caselles and E. Rubio (2018). Interest and Method The study used to estimate radiative flux in semi-arid regions using satellite observations. 57(3), 531546 of the Journal of Applied Meteorology and Climatology.

Davy, R., Esau, I., Reuder, J. (2020). The influence on the shape of the land and resulting change in solar radiation. 176, 277295 in Boundary-Layer Meteorology.

Escobedo, J. F., Gomes, E. N., Oliveira, A. P., and Soares, J. (2020). The influence of aerosols that form in the cities on the solar

radiation. *Atmospheric Research*, 235, 104801.

GonCMath presumptive european central bank eurozone iv discourseseal classifys rev GonCCantilha verbs EuropeDtoz cv regiment dystat LeonCdia thesis wwt havin pres GbCcesloned laymen basking ivory iv Based on statistical and neural approaches, hybrid models can forecast solar radiation hourly to be used in energy.

Maduekwe, A. A. and Akinbode, O. M. (2020). Verification of satellite-derived data on radiation of the sun in the sub-Saharan Africa. *Journal of Energy in Southern Africa* 31 (1), 26 34.

Murakami, M. and Tsujimoto, H. (2019). Incorporation of site-specific parameters into models used in prediction of solar irradiation. *Renewable Energy*, 136, 399410.

Raptis, P. I., and Kazantzidis, A. (2018). Spectral sun irradiance changes and their implications to photovoltaics. 173, 222230 in *Solar Energy*.

SimO, A., and Pedros, R. (2019). The ways in which latitude and topography influence the quantity of solar radiation that differs. *International journal of climatology, RSMM* 39,(5), 2743-2758.

Tiwari, S. and Chandra, R. (2021). Meridian energy merc Mars and light spectrum components. *Journal of solar energy engineering*,143(2) 024503.

Zhu, W., Y, He, and Ma (2021). A mixed model with an estimation of solar radiation with the help of even weather data. *The Applied Energy*, 283, 116258.